

A computational model of an Einstein-Solid model to study gas sorption in solid surfaces: effects on the solid wall structure

M. Lara-Peña and H. Domínguez

*Department of Physics and Astronomy, University of British Columbia, Vancouver, British Columbia, V6T1Z1, Canada. On sabbatical leave, Instituto de Investigaciones en Materiales, Universidad Nacional Autónoma de México, México, 04510 CDMX, México.
e-mail: hectordc@unam.mx*

Received 22 January 2016; accepted 3 June 2016

Sorption of carbon dioxide (CO_2) on solid surfaces is studied by a Reactive Monte Carlo (RxMC) method. A simple model of the $\text{A+B} \rightleftharpoons \text{C}$ reaction is used to mimic the experimental reactions $\text{CO}_2 + \text{Li}_2\text{O} \rightleftharpoons \text{Li}_2\text{CO}_3$. Two different solid surfaces were constructed to study sorption of the gas, a face centered cubic (FCC) and a disordered walls. In each case the solids were composed of particles with two different models, the first one consisted of rigid particles and the second model considered particles which were allowed to vibrate inside the solid with a given spring constant, *i.e.* a solid of Einstein. Density profiles analysis showed that not only physisorption but also chemisorption was observed. Comparisons of gas absorption of the two walls with a cubic simple solid structure, reported previously, were carried out and it was observed that the disordered and the cubic simple walls present similar values. However, the FCC walls produced higher absorption than the others, in particular at low temperatures.

Keywords: Surface structure; reactive simulations; absorption and adsorption; chemical reaction.

Se realizaron estudios de sorción de dióxido de carbono (CO_2) usando el método de Monte Carlo reactivo (RxMC). Usando un modelo simple $\text{A+B} \rightleftharpoons \text{C}$ se simuló la reacción $\text{CO}_2 + \text{Li}_2\text{O} \rightleftharpoons \text{Li}_2\text{CO}_3$. Los estudios se llevaron a cabo usando dos superficies distintas, un sólido cúbico centrado en las caras (FCC) y un sólido desordenado. Para ambos sólidos se utilizaron dos modelos de partículas, el primero consistió de partículas rígidas y el segundo de partículas que podían vibrar con una constante de resorte, esto es, se modeló un sólido de Einstein. Mediante los perfiles de densidad se observó no solo fisorción pero también quimisorción. Los resultados de absorción se compararon con los obtenidos, en un trabajo anterior, en un sólido formado con un arreglo cúbico simple. Tanto el sólido desordenado como cúbico tuvieron absorciones similares. El sólido FCC presentó mayor absorción que las otras paredes, en particular a bajas temperaturas.

Descriptores: Superficies; simulaciones reactivas; absorción y adsorción; reacción química.

PACS: 61.20.Ja; 61.30.Hn; 68.08.De

1. Introduction

Retention of gases on solid surfaces has been the subject of study for several years. In particular, due to the industrial implications, sorption of carbon dioxide (CO_2) on different substrates has been investigated using theory and experimental approaches. Moreover, new materials with good sorption properties such as lithium ceramics have been tested to retain CO_2 [1–5]. In fact, absorption of CO_2 can be obtained by the chemical reaction $\text{Li}_2\text{O} + \text{CO}_2 \rightleftharpoons \text{Li}_2\text{CO}_3$, *i.e.* Li_2O (lithium oxide) is highly reactive with CO_2 to form Li_2CO_3 (lithium carbonate). Therefore, few experiments have been conducted to study such reaction and a schematic view of how CO_2 is chemisorbed in Li_2O ceramics has been proposed [1].

From the theoretical point of view CO_2 sorption has been studied with density functional theories [6–8] and molecular simulations [9–13]. One of the classical approaches to study chemical reactions has been the Reactive Monte Carlo (RxMC) method. In fact, by using this methodology a model based on a solid of Einstein model for the surface was proposed by our group to understand the physics behind the reaction $\text{Li}_2\text{O} + \text{CO}_2 \rightleftharpoons \text{Li}_2\text{CO}_3$ [14]. The computational model

agreed with the experimental assumption given by previous authors [1], *i.e.* during the reaction a Li_2CO_3 shell is formed on the Li_2O surface. Then, at high temperatures that shell is cracked and free paths might be created allowing diffusion of CO_2 into the ceramic increasing its absorption in the solid.

In this paper we continue our studies of CO_2 sorption in solid surfaces given by the $\text{Li}_2\text{O} + \text{CO}_2 \rightleftharpoons \text{Li}_2\text{CO}_3$ reaction. In particular, in the present work, studies of how sorption is modified by different solid surfaces is investigated. The crystal structure of the Li_2O ceramic is reported as a cubic array, therefore in the previous simulations [14] a simple cubic surface was used to start the sorption studies of this system. However, since the actual Li_2O crystal structure is a face centered cubic (FCC) in this work we conducted simulations using a solid surface with that particular structure. In this way we can compare absorption on surfaces with cubic crystal structures. We also want to investigate if disorganized structures have better absorption properties compared with crystal structures, then a third surface was tested and a disordered surface was constructed. Then simulations were conducted and comparison among the three surfaces were carried out.

2. Computational Method and Model

Simulations were conducted in a similar way as described in a previous work [14]. A gas with low density was put inside two parallel walls separated by a distance H . The walls were constructed using an atomistic model with a FCC or a disorder structure. For the FCC walls a lattice cell of 1.1054σ was used whereas for the disordered walls random particles were located in the solid. Moreover, two models were simulated for both solid walls; in the first one the atoms in the solid were considered as rigid sites whereas in the second model they were allowed to vibrate around their equilibrium positions, *i.e.* a solid of Einstein model was constructed.

For the real chemical reaction ($\text{Li}_2\text{O} + \text{CO}_2 \rightleftharpoons \text{Li}_2\text{CO}_3$) a simple model, $A + B \rightleftharpoons C$, was used where species “A”, “B” and “C” were modeled as spherical particles interacting with a Lennard Jones potential (LJ). “A” represents the gas, “B” the Li_2O and “C” the Li_2CO_3 . The Lennard Jones parameters for each specie were taken from reference [14].

The main Monte Carlo (R_xMC) steps are (details can be found in reference [15]),

- 1) A particle “A” is chosen at random and a change in position with the standard MC probability is attempted [16].
- 2) Forward reaction. A particle “B” is chosen at random and it is changed to particle “C”. At the same time a particle “A” is removed from the system. Then, the move is accepted with probability of $\min[1, P_{r \rightarrow s}^+]$
- 3) Reverse reaction. A particle “C” is chosen at random and it is changed to particle “B”. At the same time a particle “A” is randomly created in the gas phase. Then, the move is accepted with probability of $\min[1, P_{s \rightarrow r}^-]$.

The transition probability $r \rightarrow s$ is given by,

$$P_{r \rightarrow s} = e^{-\beta \delta U_{rs}} \prod_{i=1}^n q_i^{\nu_i} \prod_{i=1}^n \frac{N_i!}{[N_i + \nu_i]} \quad (1)$$

$\beta=1/KT$ (K the Boltzmann constant and T the temperature), δU_{rs} is the energy change from state r to s , q_i is the partition function, N_i is the number of particles of type i , ν_i is the stoichiometric coefficient of component i and n is the number of components [15]. The reverse reaction transition probability ($s \rightarrow r$) is obtained by replacing ν_i by $-\nu_i$.

From the chemical equilibrium condition equation 1 is written as

$$P_{A+B \rightarrow C}^+ = \frac{q_C}{q_A q_B} \frac{N_A N_B}{N_C + 1} e^{-\beta \delta U} \quad (2)$$

and the reverse reaction,

$$P_{C \rightarrow A+B}^- = \frac{q_A q_B}{q_C} \frac{N_C}{(N_A + 1)(N_B + 1)} e^{-\beta \delta U'} \quad (3)$$

In the last equations, q_A , q_B and q_C are the individual partition functions which have the contributions of all degrees of freedom, $q_A = q_{t_A} q_{v_A} q_{r_A}$ with q_{t_A} the translational contribution, q_{v_A} the vibrational contribution and q_{r_A} includes the

rotational, electrical and nuclear contributions. In all simulations q_{r_i} was considered as unity and since only particles of type “A” are allowed to translate, then

$$q_{t_A} = V \left(\frac{2\pi m_i K T}{h^2} \right)^{3/2} \quad (4)$$

with V the volume, h the constant of Planck and m the mass. As it is common in computer simulations we used reduced units (with the first specie “A”), then the probabilities can be written as,

$$P_{A+B \rightarrow C}^+ = \frac{V^{*-1} T^{*-3/2}}{\Lambda} \frac{N_A N_B}{N_C + 1} e^{-\delta U^*/T^*} \left(\frac{q_{v_C}}{q_{v_B}} \right) \quad (5)$$

$$P_{C \rightarrow A+B}^- = V^* T^{*3/2} \Lambda \frac{N_C}{(N_A + 1)(N_B + 1)} \times e^{-\delta U'^*/T^*} \left(\frac{q_{v_B}}{q_{v_C}} \right) \quad (6)$$

where the usual reduced units were used, *i.e.* $V^*=V/\sigma_A^3$, $T^*=KT/\epsilon_A$, $U^*=U/\epsilon_A$ and with $\Lambda=(2\pi m_A \epsilon_A \sigma_A^2/h^2)^{3/2}$.

Equation 5 and 6 with $q_{v_A} = q_{v_B} = 1$ are used to simulate the rigid model [14].

For the second model the vibrate partition function, of particles “B” and “C”, was written as $q_v = \sum_n e^{-\beta E_n}$ with $E_n = \hbar\omega(n + 1/2)$ where $\hbar = h/2\pi$ and ω the particle frequency [17]. With the approximation $KT \gg \hbar\omega$, the partition functions can be written as $q_{v_B} \approx KT/\hbar\omega_B$ and $q_{v_C} \approx KT/\hbar\omega_C$. By using the relation $\omega_i = \sqrt{k_i/m_i}$ (k_i , the spring constant) Eqs. 5 and 6 can be rewritten as [14],

$$P_{A+B \rightarrow C}^+ = \frac{V^{*-1} T^{*-3/2}}{\Lambda} \frac{N_A N_B}{N_C + 1} e^{-\beta \delta U} \left(\frac{k_B m_C}{k_C m_B} \right)^{3/2} \quad (7)$$

$$P_{C \rightarrow A+B}^- = V^* T^{*3/2} \Lambda \frac{N_C}{(N_A + 1)(N_B + 1)} \times e^{-\beta \delta U'} \left(\frac{k_C m_B}{k_B m_C} \right)^{3/2} \quad (8)$$

It is important to note that Eqs. 7 and 8 cannot be used for zero spring constants since they will be undefined.

All simulations were conducted in the NVT ensemble. For the disordered walls the box dimension were $X = Y = 9.0281$ and $Z = 600$ and they started with 1200 particles of type “A” and 1452 particles of type ”B”. For the FCC walls, $X = Y = 9.2115$ and $Z = 577$ and the simulations started with 1200 and 1440 particles of species “A” and “B”, respectively. Periodic boundary conditions were used in the X - Y directions only and it was used a cutoff radius of $4.0\sigma_A$. In order to keep the solid layer structure the particles in the walls were allowed to move in X-Y directions only. Typical simulations considered runs of 10000 MC steps for equilibration and another 40000 MC steps for data production. Configurational energy was monitored during the simulations to determine when the systems reached equilibrium (when energy did not have significant variations). All simulations were

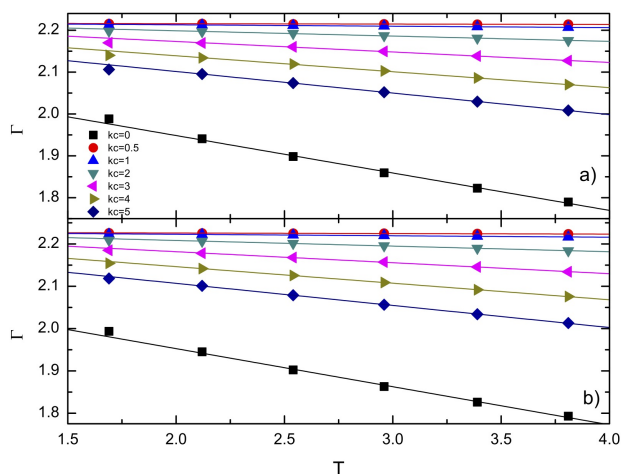


FIGURE 1. Sorption curves as a function of the temperature for different k_c . The solid lines are the best fitting. Data with $k_c = 0$ are calculated with the rigid model whereas the others (k_c) were calculated with the Einstein model.

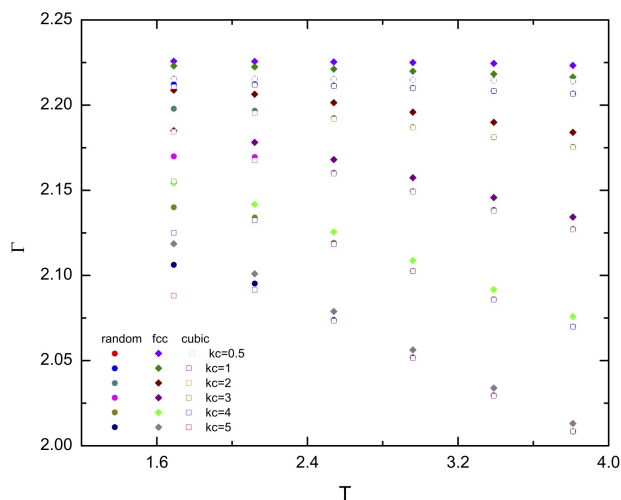


FIGURE 2. Sorption curves as function of the temperature for the Einstein model. Simulations for the FCC, the disordered and the cubic simple walls are shown. Symbols are given in the figure for different values of the spring constant k_c .

conducted for $\Lambda = 0.001$ with $k_B = 5$ and the value of k_c was changed. For the rest of the paper all quantities are given in reduced units.

3. Results

Simulations were carried out for different values of spring constants, k , and since the reduced critical temperature for a Lennard Jones fluid is $T = 1.25$ [18] those simulations were carried out at reduced temperatures above $T = 1.5$.

3.1. sorption

In Fig. 1 the absorption curves of the gas (specie A) as function of the reduced temperature for the disordered and the

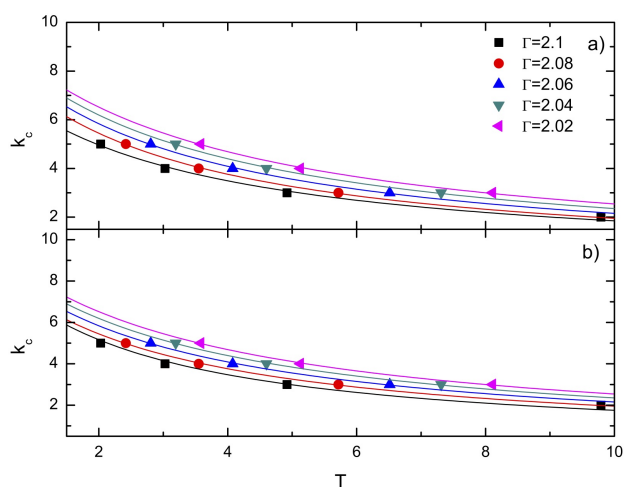


FIGURE 3. Spring constants, k_c , as function of the temperature for different sorption values, Γ . The fitting “a” and “b” parameters (in equation 9) are: a) For disordered walls, 0.1165 and 0.0425 (black), 0.1014 and 0.0411 (red), 0.0982 and 0.0366 (blue), 0.0955, 0.0329 (green), and 0.0934 and 0.0299 (pink), respectively. b) For FCC walls, 0.1135 and 0.0415 (black), 0.1004 and 0.0398 (red), 0.0969 and 0.0358 (blue), 0.0939, 0.0325 (green), and 0.0916 and 0.0298 (pink), respectively.

the FCC walls are shown. Here absorption was defined as $\Gamma = m_f/m_i$, with m_f and m_i the total initial and final masses in the solid, respectively. As a general trend the rigid models present significant lower absorption than the Einstein model. Moreover, it is noted that chemisorption increased as the spring constant, k_C , decreased. From these results it seems that the presence of a spring in the solid particles modified the substrate absorption.

For the disordered surface it is observed similar absorption from $T = 1.5$ to $T = 2.0$, then it decreased linearly (Fig. 1a). For the FCC surface absorption had always a linear decayed with the temperature (Fig. 1b). It is also noted that FCC walls have slightly higher absorption than the disordered walls at the same temperature. In Fig. 2 absorption curves of both walls are compared with the absorption in a simple cubic wall. The values for the cubic wall were in good agreement with those reported in a previous work [14]. In the figure is noted that FCC walls produced more absorption than the disordered and cubic walls for all the simulated temperatures. Moreover, the disordered and cubic walls had similar data. At low temperatures there was a higher difference in the absorption and as the temperature increased that difference became smaller. It is also interesting to observe a maximum in the curves between temperatures $T = 1.6 - 2.5$ for the cubic walls, however, that maximum disappeared for the other walls.

As in the previous paper, it was determined the behaviour of the spring constant as function of the temperature for a given absorption in the Einstein solid model (Fig. 3). For both surfaces, the disordered and the FCC, it was found an inverse dependence of the spring constant with the temperature,

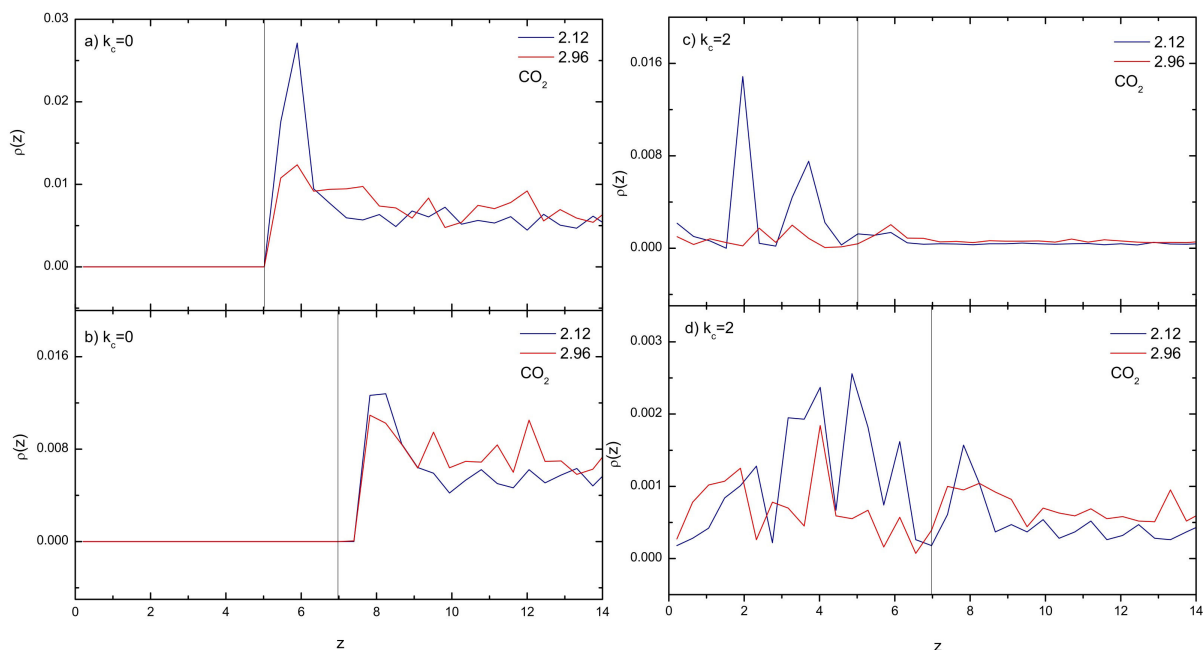


FIGURE 4. Typical density profiles for the gas particles (specie A) at different spring constants at two different reduced temperatures $T = 2.12$ (blue lines) and $T = 2.96$ (red lines). a) $k_c = 0$ with disordered walls, b) $k_c = 0$ with FCC walls, c) $k_c = 2$ with disordered walls, d) $k_c = 2$ with FCC walls. The position of the substrate in each case is shown by the black line.

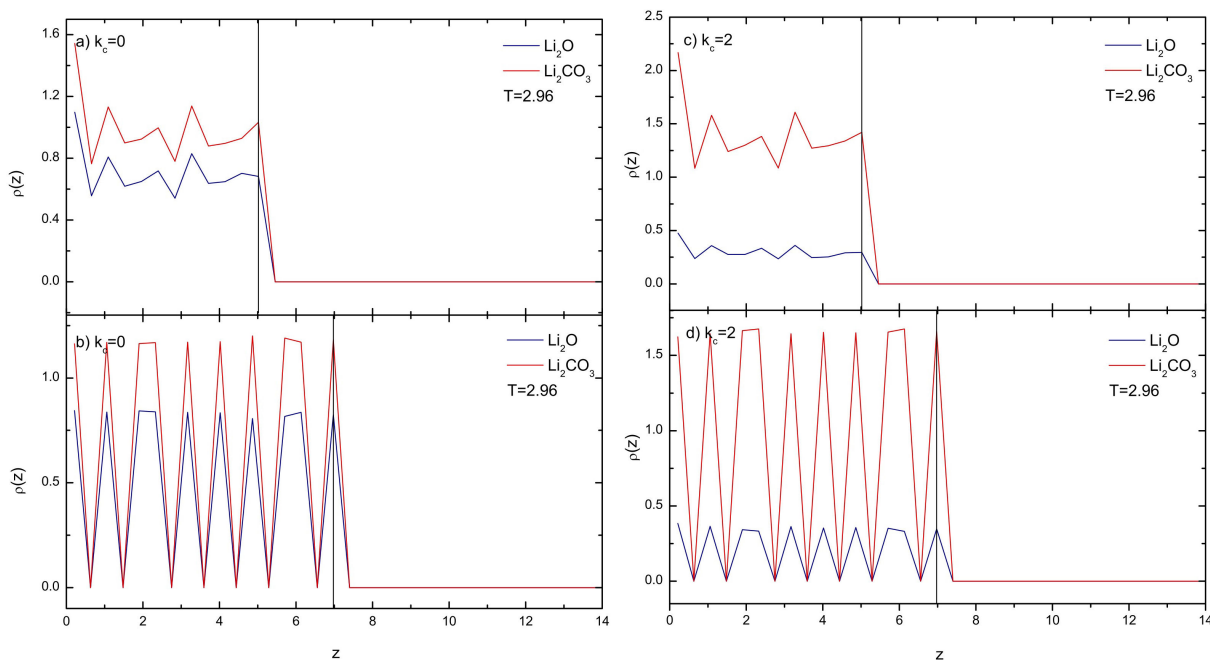


FIGURE 5. Typical density profiles for the solid particles at different spring constants at $T = 2.96$. Blue lines for the specie B and red lines for the specie C. a) $k_c = 0$ with disordered walls, b) $k_c = 0$ with FCC walls, c) $k_c = 2$ with disordered walls, d) $k_c = 2$ with FCC walls. The position of the substrate in each case is shown by the black line.

$$k_c(T) = \frac{1}{a + bT} \quad (9)$$

Moreover, both walls had similar fitting parameters “a” and “b” (see Fig. 3).

3.2. Structure

The structure of the different particles in the reaction were studied in terms of density profiles along the Z-direction, *i.e.* perpendicular to the surfaces. The structure of the gas parti-

cles close to the surfaces present different features as noted in Fig. 4. For instance, for the rigid solid model (first model, $k_c = 0$) we did not observe any particles inside any of the solid surfaces, *i.e.* the gas was adsorbed at the solid-gas interface (Fig. 4a and 4b). On the other hand, the system with disordered walls (Fig. 4a) had a stronger structure close to the surface at low temperature ($T = 2.12$) than the system with FCC walls (Fig. 3b) suggested by the first high peak in the density profile. On the other hand, for the Einstein solid model the gas particles penetrated into the solid region (Fig. 4c y 4d). In fact, a strong structure inside the FCC walls at low temperature ($T = 2.12$) was observed for the gas particles. In the case of the disordered walls the structure was also strong however, less number of peaks were formed. It seems that the vibration of the solid particles in the model with springs created gaps which allow the fluid molecules (specie A) to move inside the solid by enhancing the sorption. From those results not only absorption but also adsorption was observed in the simulations.

The structure of particles inside the solid walls (species B and C) were also analyzed. For the disordered walls the B (Li_2O) and C (Li_2CO_3) particles were distributed uniformly along the surface regardless the value of the spring constant (see *e.g.* Fig. 5a and 5c). On the other hand, for the FCC walls the B and C particles kept the FCC layer array (Fig. 5b and 5d). Despite the height of the peaks in the density profiles similar trends were depicted for all the spring constants (k_c). However, it was noted that the profiles for the C particles were always higher than those of the B particles, for the disordered and FCC walls, suggesting that in all cases absorption of gas particles was favored by the walls.

3.3. Conclusions

Sorption of gas molecules on two different walls structures were studied by using a reactive Monte Carlo method

(RxMC); a FCC and a disordered wall. For each wall two models for the solid particles were employed, a rigid model (solid particles were fixed) and an Einstein solid model (solid particles were allowed to vibrate). For both walls it was found an inverse function dependence of the spring constant with the temperature.

The FCC walls present slightly more absorption than the disorder ones regardless if the rigid or the Einstein solid models were used. Moreover, the FCC walls also present higher absorption than the simple cubic walls at the same temperature and at the same spring constant. Since the packing factor in a FCC (0.74) cell is higher than that in the simple cubic (0.52), *i.e.* there are more atoms per unit cell in the FCC in the first wall than in the second one. Therefore, there are more solid atoms to react with the gas by producing more absorption. Then, this feature combined with the use of a spring constant in the solid particles seem to enhance absorption in solid surfaces.

Right now only three different surfaces have been tested to study gas sorption on a solid surface with our model and the results suggest that the surface with the higher packing fraction shows better absorption. However, it is not possible to generalize that FCC surfaces have the best absorption properties since comparisons with other surfaces, with different structures, should be done to corroborate this issue and to have a more general conclusion.

Acknowledgments

The authors acknowledge DGTIC-UNAM for the supercomputer facilities. HD acknowledges support from Conacyt-Mexico and DGAPA-UNAM-Mexico for sabbatical scholarships. ML-P acknowledges the postgraduate scholarship from Conacyt-Mexico.

1. H. A. Mosqueda, C. Vazquez, P. Bosh, H. Pfeiffer, *Chem. Mater.* **18** (2006) 2307.
2. S. Shan, *et al.*, *Ceram. Int.* **39** (2013) 5437.
3. M.T. Dunstan, W. Liu, A.F. Adriano *et al.*, *Chem. Mater.* **25** (2013) 4881.
4. T. Avalos-Rendon, V.H. Lara, H. Pfeiffer, *Ind. Eng. Chem. Res.* **51** (2012) 2622.
5. B.N. Nair, T. Yamaguchi, H. Kawamura, S.I. Nakao, K. Nakagawa, *J. Am. Ceram. Soc.* **87** (2004) 68.
6. B. Zhang, A.C.T. van Duin, J.K. Johnson, *J. Phys. Chem. B.* **118** (2014) 12008.
7. Y. Duan *et al.*, *Aerosol Air Qual. Res.* **14** (2014) 470.
8. L. Yue, W. Lipinski, *Int. J. Heat Mass transfer.* **85** (2015) 1058.
9. A. Nalaparaju *et al.*, *Chem. Eng. Sci.*, **124** (2015) 70.
10. A.A. Sizova, V.V. Sizov, E.N. Brodskaya, *Colloid. J.* **77** (2015) 82.
11. Z. Jin, A. Firoozabadi, *Fluid Phase Equilib.* **382** (2014) 10.
12. L. Huang, *et al.*, *Phys. Chem. Chem. Phys.* **14** (2012) 11327.
13. H. Dominguez, *Rev. Mex. Fis.* **58** (2012) 378.
14. M. Lara-Peña and H. Dominguez, *Pys. Chem. Chem. Phys.* **17** (2015) 27894.
15. J.K. Johnson, A.Z. Panagiotopoulos, K.E. Gubbins, *Molec. Phys.* **81** (1994) 717.
16. M. P. Allen and D. J. Tildesley, *Computer Simulations of Liquids* (Clarendon Press, Oxford, 1993).
17. D. A. MacQuarrie, *Statistical Mechanics* (Harper and Row 1976).
18. J.K. Johnson, J.A. Zollweg, K.E. Gubbins, *Molec. Phys.* **78** (1993) 591.